



## Charge Carrier Mechanism in CdTe/ZnTe Core/Shell Nanocrystals for Photoelectrodes by Laser Ablation Method

Akeel M. Kadim<sup>1,\*</sup>, Amjed M. Shareef<sup>1</sup>

Department of Medical Physics, College of Applied Medical Sciences, University of Kerbala, Kerbala, Iraq.

### Article's Information

Received: 30.05.2025  
Accepted: 10.09.2025  
Published: 15.12.2025

### Keywords:

CdTe  
ZnTe  
Core/Shell  
Optical properties  
Laser ablation

### Abstract

Laser ablation techniques employing photo/thermosensitive materials were used to synthesize and characterize CdTe/ZnTe core/shell nanocrystals (NCs) or quantum dots (QDs). Upon excitation by a laser pulse (Nd: YAG laser with 150 pulses and 600 mJ of power), a broad signal indicating ground state bleach in the core/shell nanocrystals was observed in the transient absorption spectrum, which was compatible with the absorption spectra. These photoelectrodes were pre-sensitized by CdTe/ZnTe core/shell NCs that were deposited utilising an FTO/TPD/CdTe-ZnTe/PEDOT: PSS/Ag scaffold of a certain thickness on a transparent glass-substrate FTO (Fluoride tin oxide). According to PL measurements, the energygap ( $E_g$ ) of CdTe/ZnTe core/shell NCs is around 2 and 2.5 eV for CdTe-core and ZnTe-shell respectively from Tauc relation. A current-voltage (I-V) characteristic, in addition to lighting at 3V, verifies an ideal environment and formation. A laser ablation-produced CdTe/ZnTe core/shell NCs improved the photoelectrodes' performance by improving the carrier's charge mobility and, therefore, recombination processes inside the NCs along with TPD and PEDOT: PSS polymer ions. The development of the photoelectrode device's increasing interaction with PEDOT: PSS and TPD ions regarding core/shell NCs to use limited voltages and provide desirable light output may cause a bias in forward current flow.

<http://doi.org/10.22401/ANJS.28.4.13>

\*Corresponding author: [akeel\\_a86@yahoo.com](mailto:akeel_a86@yahoo.com)



This work is licensed under a [Creative Commons Attribution 4.0 International License](https://creativecommons.org/licenses/by/4.0/)

### 1. Introduction

The quantum-confined nature of semiconductor nanocrystals (NCs) or quantum dots (QDs) makes them fundamentally intriguing and offers enormous promise for use in solar cells, light-emitting devices, biological images, and photocatalysis. With the ability to modify the materials of the core and shell to modify the charge carrier localization, core/shell NCs offer more flexibility in charge carrier confinement [1-2]. The Type-I structure, for instance, has both electrons and holes confined in the core, while the Type-II structure has alignment of the core and shell's stagger bands, which causes the electrons and holes to be spatially separated. Decoupling between electrons and holes gives systems of type-II nanocrystals their extended radiant lifetimes, making them more suitable for photoelectrode system applications [2,3]. With a bandgap of 1.5 eV, CdTe-based NCs show promise as photoelectrode device candidates. The dynamics of carriers in

CdTe/ZnTe NCs with a high density of surface trap states that were synthesized in the aqueous phase at low temperatures were previously examined by [1,3]. However, high-quality NCs with a lower trap density are required for photoelectrode devices. The kinetics of ultrafast excitons in CdTe/ZnTe core/shell NCs synthesized by chemical techniques have been examined here using transient absorption (TA) spectroscopy [3]. Furthermore, CdTe/ZnTe NCs are a potential material for photoelectrode device applications because of the continued absorption and charge separation brought about by the core/shell structure [3,4]. The improved optoelectronic capabilities of these NCs are implied by their increased comparison the photoluminescence lifetime and quantum yield to the CdTe core. Because of the type-II character, which involves the electron-hole being separated from one another, the core/shell NCs in TA tests displayed signs of charge separation. Importantly, the enhanced surface passivation was

shown to be consistent with a significantly slower rate of recombination in the core/shell NCs. We created sensitised solar cell devices using the synthesized NCs as a proof-of-concept [4-5]. However, crystalline imperfections in sensitising QDs significantly increase the improper electron-hole recombination, which is the primary cause of several limitations in photoelectrode devices (QDPDs). It is generally known that these defects can develop inside semiconductor NCs, especially on their surface, due to the small size of the crystalline lattice [6]. A polymer that conducts Poly(3,4-ethylenedioxythiophene) polystyrene sulfonate (PEDOT: PSS) (electron transport layer) and poly(N,N'-bis-4-butylphenyl-N,N'-bisphenyl) benzidine (TPD) (hole transport layer) with acceptance levels to examine the influence of form on electrochemical and optical characteristics [5-6]. Some localised levels of electron energy in QDs' bandgap energy, referred to as the trap states, can be produced by the incomplete dangling bands. These energy levels have the potential to decrease efficiency by introducing novel transition pathways for electrons and holes that are not preferred in QDPDs [7]. In luminous NCs, the aforementioned issue was previously examined and resolved, leading to increased photoluminescence quantum yields. This was accomplished by applying a few organic and inorganic shells to the NC's surface. The associated electronic energy states may be eliminated and the surface dangling bonds passivated by the shell formation [8]. In hybrid quantum dot photoelectrode devices (QDPDs), this resulted in a strong and even utilised for sharp emissions, with a narrow band-edge emission. PL quantum yields of 90% have been reported for the synthesis of core-shell NCs, such as CdS/CdSe, CdSe/CdS/ZnS, and CdSe/CdS NCs [9]. The electron-holes in these devices are split between the core and shell regions due to the band-edge positions of the core and shell materials. It follows that this technique may be as effective in raising QDPDs' power conversion efficiency. Unsuitable electron-hole recombination might be reduced; the voltage and density of current that resulted could be greatly increased [10]. However, for the efficient transitions between electrons and holes in QDPDs, the shell thickness and assignments of the core/shell NCs' band-edges should be designed appropriately. To boost the efficacy of light harvesting, co-sensitization could be carried out concurrently [11]. The production of NCs with colloidal core/shell as enhanced illumination sensitizers in QDPDs has been the subject of numerous studies. The aqueous methods have been used to synthesise these NCs [12]. Wet synthesis of core/shell NCs could be widely used

due to its easy synthesis process and low-cost, low-toxic materials. Meanwhile, the crystalline nature of the QDs has defects and trap states are created [13]. Chemical precipitation was used to synthesise the core/shell utilising laser ablation techniques, and photo or microwave-activated techniques employing photo/thermosensitive materials were used to create the shells [13-14]. However, additional research on various core-shell NC types with various optoelectronic characteristics and their uses in QDPDs is still very much in the future.

Here, we present the optical and photovoltaic characteristics of colloidal CdTe/ZnTe core/shell QDs synthesized by laser ablation for use in quantum dot photoelectrode devices (QDPDs). The CdTe/ZnTe core/shell determines by UV-vis absorption, PL spectra, and I-V characteristics of such NCs, the detected charges and carriers' potential physical mechanism influences the outcomes of CdTe/ZnTe core/shell NC systems. The photoelectrode device's progressive interaction development about core/shell NCs with TPD ion and PEDOT: PSS may lead to a bias in forward current flow in order to use restricted volts and obtain favorable results for light output. This innovative approach could enhance the overall efficiency of light-emitting applications, paving the way for improved energy conversion rates. Future experiments will further explore the optimal configurations of the core/shell nanocrystals to maximize performance.

## **2. Materials and Methods**

### **2.1. Preparation of Cadmium Telluride Nanocrystals (CdTe NCs)**

The Fluka Company supplied all of the primary chemicals, which were used without additional purification. Initially, 30 millilitres of deionised water were used to dissolve 0.6 grams of cadmium chloride ( $\text{CdCl}_2$ ) and 0.2 grams of sodium telluride ( $\text{Na}_2\text{Te}$ ). After two hours of stirring in a container designed to produce homogenous nanocrystals, the cadmium telluride (CdTe) nanocrystal solution was passed, causing its colour to shift to a light green. After five rounds of cleaning with deionised water, the cadmium telluride (CdTe) nanocrystals were vacuum packed.

### **2.2. Preparation of Zinc Telluride Nanocrystals (ZnTe NCs)**

In the same way. Twenty millilitres of deionised water ( $\text{Na}_2\text{H}_2\text{Te}$ ) were used to dissolve 0.9 grams of zinc chloride ( $\text{ZnCl}_2$ ) and 0.2 grams of sodium telluride ( $\text{Na}_2\text{Te}$ ). Before passing the nanocrystal solution, a container was rotating to create uniform nanocrystals and stirring for an hour. This caused

the ZnTe NCs solution's colour to shift to a light green. After five rounds of cleaning with deionised water, the ZnTe NCs were vacuumed packed.

### 2.3. Preparation of CdTe/ZnTe Core/Shell NCs

Using a 1:2 molar ratios, 10 ml of the CdTe combination and 20 ml of the ZnTe/NCs solution were combined in a flask to create the CdTe/ZnTe core/shell NCs. It seems to be utilised to synthesise CdTe/ZnTe nanocrystals using the Nd: YAG laser, which operates at 1064nm (see in Fig. 1). A lens distance of 7 cm is employed to focus the laser beam focal length 15 cm on the mixed solution. The colour of the CdTe/ZnTe NCs mix changed to bright green-yellowish colouration as a result of a container that rotated to create uniform nanocrystals and was agitated for two hours ahead of passing away the nanocrystal mix. The CdTe/ZnTe core/shell NCs were then gathered, washed four times using deionised water.

### 2.4. Fabrication of Photoelectrode of CdTe/ZnTe Core/Shell NCs

Three layers were used in the subsequent production of photoelectrode CdTe/ZnTe core/shell NCs. These

layers are currently composed of PEDOT: PSS conductive polymer, TPD polymer, and CdTe/ZnTe core/shell NCs, which are deposited on the FTO substrate in that order. A polymer that conducts Sigma-Aldrich provides poly(3,4-ethylene-dioxythiophene) polystyrene sulfonate (PEDOT: PSS) and poly(N,N'-bis-4-butylphenyl-N,N'-bisphenyl) benzidine (TPD). By using an aggregation approach that involves masked rotation at 3000 rotations per minute. for approximately 5-12 seconds for independently covered, an organic polymeric coating that melts 20 mg/ml in ethanol is injected into a glass substrate. TPD polymer was utilised in the cover as the first layer to prevent crashes, followed by CdTe/ZnTe core/shell NCs in the second layer and PEDOT: PSS conductive polymer in the third. After coating Each cover's coating is removed after ten minutes at 55 °C. The CdTe/ZnTe core/shell NCs cover had a thickness of 10 nm, whilst the TPD and PEDOT: PSS polymer layers seemed to 25 and 15 nm thick, respectively. The system layer is then applied to a silver (Ag) cathode. A generator that produces electricity composed of nanostructure content that might transfer carrier charges to a nanomaterial layer in order to produce electrical watts.

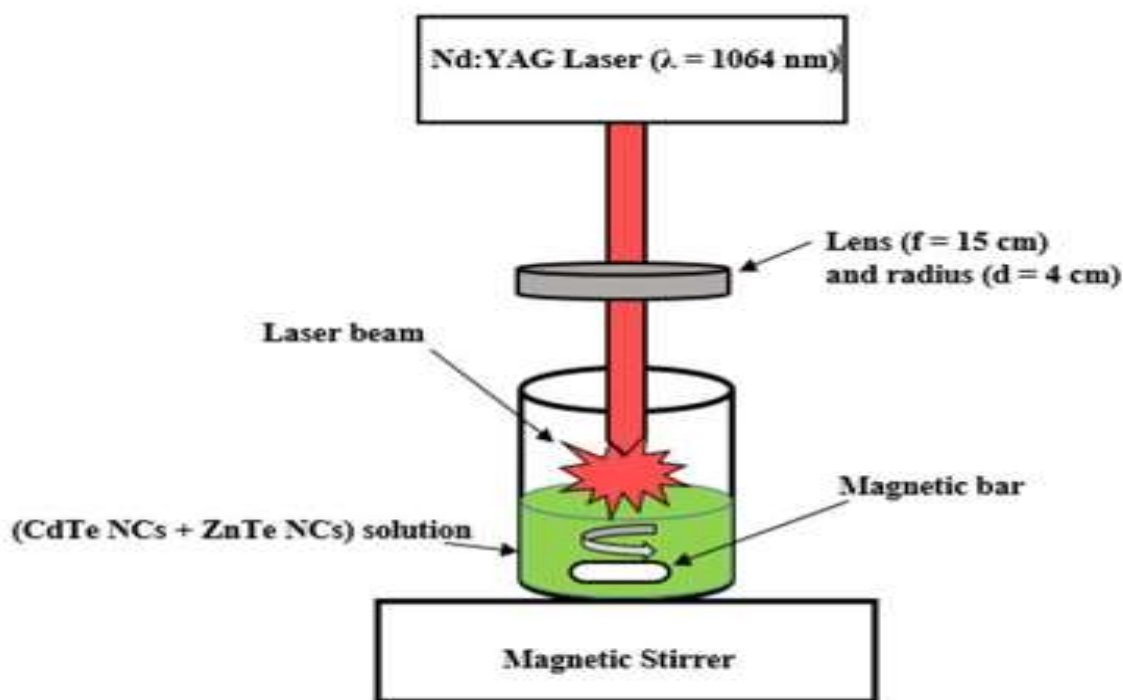


Figure 1. CdTe/ZnTe core/shell NCs colloidal production via laser ablation.

### 3. Results and Discussion

#### 3.1. Optical Measurements

The ZnTe shell and CdTe core's mismatched band alignment makes Core/shell NCs of CdTe/ZnTe are a type-II system. As a result, the system will be spatially dissociated, with the electron located within the ZnTe shell's hole and the CdTe core. UV-vis absorption spectra of the core/shell NCs of CdTe/ZnTe are shown in figure 2.

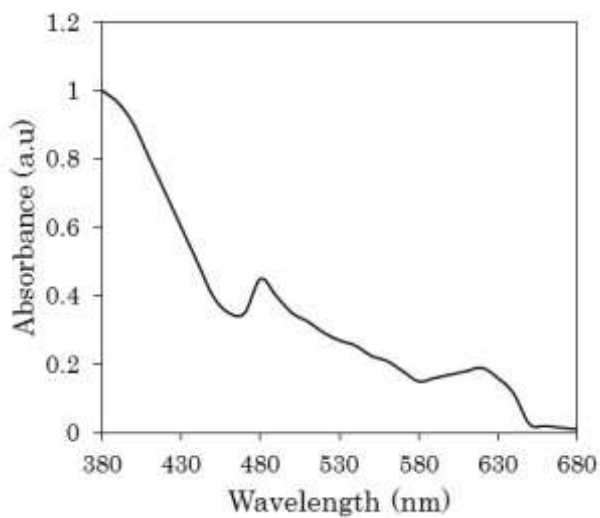


Figure 2. Absorption spectrum of CdTe/ZnTe core/shell NCs.

Additionally, type-II structure development is indicated by spectra of wide absorption with hazy excitonic characteristics. The redshift of the absorption edge from 400 to 600 nm was evident. There are two inflection points, as the image shows [3,14]. The first one is located between 480 and 620 nm. These two points of inflection are associated with the forbidden gap the shallow band created by the incomplete ZnTe NC shell and CdTe core NCs. These findings surfaced in a setting that was acceptable in relation to the absorption spectra of other researchers [15]. Following the shell's deposition, figure 3 shows that photoluminescence (PL) maxima have redshifted, signifying the creation of the core/shell structure [3,15]. This displays a particular conduction in the energy bands that is regulated at

480 and 620 nm. The near-band boundary of the emission from the ZnTe shell and the CdTe core NCs caused by free exciton recombination results in an excessive fluorescence [15-16]. The first component results from radiative recombination, whereas the second is caused by shallow trap-mediated recombination. Deep-level emissions are connected to these wide emissions. releases, which may result from weaknesses in construction [16]. Photoluminescence must have shown that the energygap in CdTe/ZnTe core/shell NCs from Tauc relation ( $\lambda$  (nm)=1240/ $E_g$  (eV)) was around 2 eV for CdTe core NCs and 2.5 eV for ZnTe shell NCs.

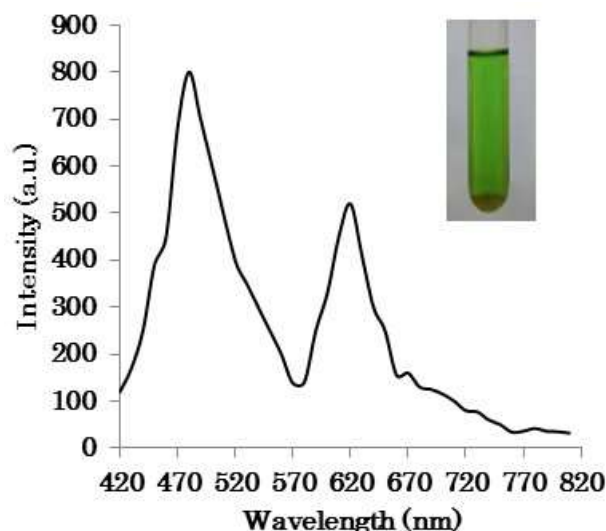


Figure 3. Photoluminescence spectrum of CdTe/ZnTe core/shell NCs.

#### 3.2. Structural Measurements

As seen in Fig. 4, a surface morphology of the generated CdTe/ZnTe NCs was seen in the SEM at 5 Kx magnification. It is evident that these NCs have a roughly spherical shape and are typically about 5 nm in size. In addition, the size distribution is broad and the particles are synthesized uniformly. In accordance with the ZnTe shell- causing it, the synthesized core/shell NCs were displayed as CdTe core. In the photoelectrodes of the CdTe/ZnTe core/shell NCs sensitised device, these NCs were used as the co-sensitizer. At a size of 500 nm, figure 4 shows a spherical shape created by QDs.

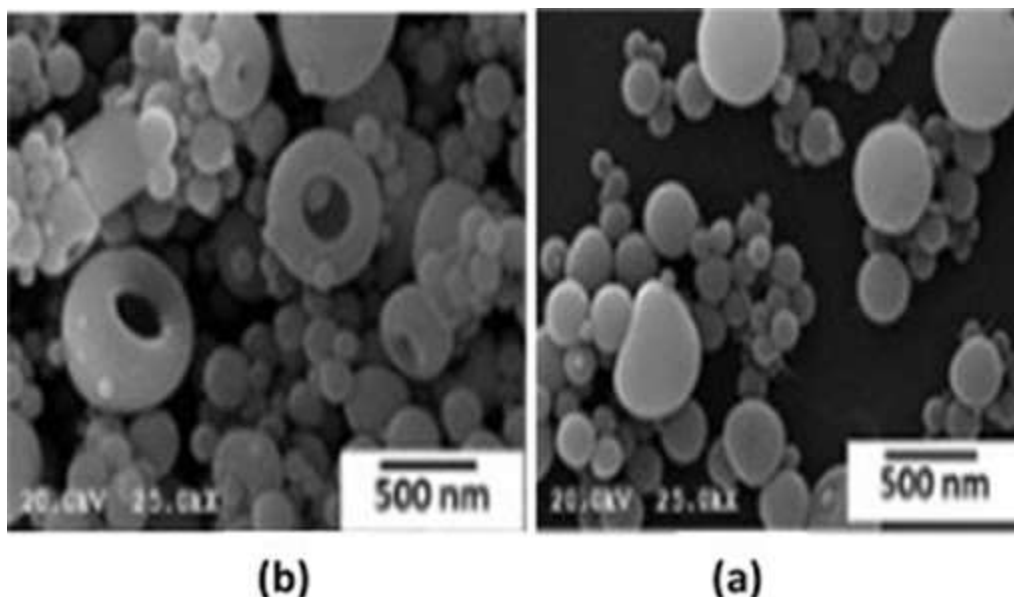


Figure 4. Core/shell scanning electron microscopy (SEM) of CdTe/ZnTe NCs colloidal precursors containing different concentration (a) 8% and (b) 2%.

### 3.3. Electrical Measurements

Using the FTO/TPD/CdTe-ZnTe/PEDOT: PSS/Ag performance, the I-V characteristics of the CdTe/ZnTe core/shell NCs photoelectrode device are displayed in figure 5. With a current of somewhat more than 0.01-1 mA and a typical convert voltage of 3 V voltage bias, figure 5 illustrates the rearrangement capability.

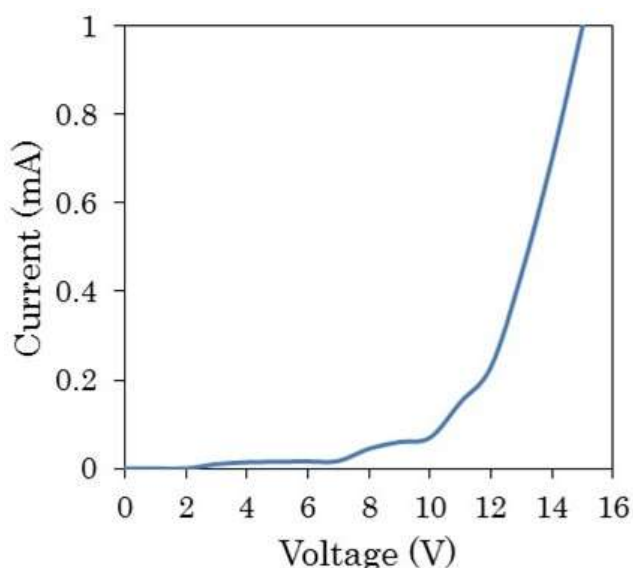


Figure 5. I-V characteristic of the quantum dot photoelectrodes devices (QDPDs).

A current-voltage analysis of a quantum dot photoelectrodes (QDPDs) product shows a depletion-

edge layer's size has decreased along with an overall increase in the current induced [11,17]. The dynamically produced current via the photoelectrode device will be greatly increased due to a sharp increase in the dispersion of holes and electrons (CdTe/ZnTe core/shell and PEDOT: PSS), which will cause the propagation band barrier to drop in both conduction and valence bands given the forward bias [17]. This can be explained by electron-hole decoupling due to the device's CdTe/ZnTe core/shell NCs configuration. The overlap of the electron-hole wave function is necessary for the recombination process, which is known as Auger-assisted energy transfer. The hole moves between the ZnTe shell and the CdTe core as a result of the staggered band alignment in CdTe/ZnTe core/shell NCs, which minimizes the overlap. Because of ZnTe shell's surface passivation, the excitons in the core/shell NCs have a longer useful life. The CdTe/ZnTe core/shell NCs' potential as a sensitizer material for quantum dot photoelectrode devices (QDPDs) has been investigated. The PEDOT: PSS-conductive polymer counter electrode electrolyte was used to assemble the core/shell NC-sensitive TPD-organic polymer photo-anodes in order to characterise the photoelectrode device using I-V measurements [17-18]. This suggests that the ZnTe shell's surface passivation keeps the core/shell NCs steady when the TPD and PEDOT: PSS polymer electrolyte is present. Furthermore, the overgrown area's low thickness ZnTe shells results in poor passivation of the CdTe cores' surface. Consequently, the CdTe core bandgap

still contains a significant trap state density, including extremely deep trapping states. The traps' associated electron-energy levels might easily recombine a confined electron-holes within the CdTe NC core, lowering the open circuit voltage of the staying photoelectrode devices [18]. The surface passivation is more thorough in the CdTe/ZnTe core/shell NCs when overall shell size is increased. This is consistent with the fact that the efficiency increased for the NCs produced in longer shell shape durations. The trap state density in CdTe cores is reduced in this case, and some deep trap states are eliminated. Additionally, ZnTe shells' conduction band edge shifts to the lower values, resulting in a matching band gap that becomes. These could reduce the likelihood of back recombination of electrons in layers with hole in CdTe core NCs and electron-hole recombination through the fundamental NCs' trap indicates. The aforementioned factors may cause the manufactured photoelectrode devices associated open circuit voltage to rise [18-19]. These events first occur, leading to a number of processes that affect the output of the photoelectrode device; a carrying It's unclear if another synthesis is in charge of the process. A band-gap in the semi-conductors that are supplying current to other devices delivery is another factor that influences a subsequent event [20]. Within the limits of gap charges, these tools are categorised as boundary configurations, output recombination, barrier annealing, imperfections and surface imperfections. A view of an FTO/TPD/CdTe-ZnTe/PEDOT: PSS/Ag quantum photoelectrodes device is clearly visible in Figure 6, and the light emitted by this photoelectrodes device component is shown in Figure 7.



Figure 6. A picture of the FTO/TPD/CdTe-ZnTe/PEDOT: PSS/Ag photoelectrodes devices.

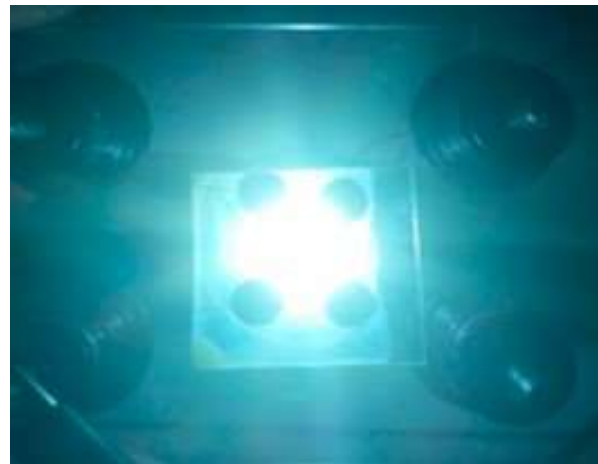


Figure 7. Light illumination produced by FTO/TPD/CdTe-ZnTe/PEDOT: PSS/Ag photoelectrodes devices.

#### 4. Conclusions

Laser ablation technique was used to synthesise core/shell NCs of CdTe/ZnTe with type-II band orientation. The creation regarding the structure of type-II redshifts the steady-state emission and absorption within the core/shell structure, increasing the PL duration and efficiency. Spectroscopic investigations of ultrafast transient absorption revealed evidence of distinct charges as the rate of electron cooling slowed due to electron-hole decoupling. Additionally, the recombination was slower in the NC's core/shell, indicating a significance of ZnTe passivation of the substrate. The performance of the photoelectrode devices was improved by CdTe/ZnTe core/shell NCs by enhancing the carrier's charge mobility and, as a result, the modes of interaction inside the ions of core/shell NCs other than TPD with PEDOT: PSS organic conductive polymer. This improvement leads to greater efficiency in energy conversion, making these core/shell nanocrystals a promising material for future photovoltaic applications. Additionally, the enhanced charge transport properties could pave the way for more advanced electronic devices. Additionally, conductive polymers and semiconductor nanoparticles form a complex when TPD and PEDOT: PSS conductive polymers are used in photoelectrodes with CdTe/ZnTe core/shell NCs semiconductor layers. This leads to high-performance photoelectrode device efficiency. Thus, the sufficient contact between the TPD, PEDOT: PSS, and core/shell NCs layer after layer can be explained by the enhanced strongly biased forward current. The characteristic of current and voltage are exactly in line, and the allocated necessary voltage has

important implications for the photoelectrode system's functionality. In order to use limited volts and achieve advantageous results for light output, the photoelectrode device's progressive interaction development about core/shell NCs with TPD ion and PEDOT: PSS might result in a bias in forward current flow. This creative method may boost light-emitting applications' overall efficiency and open up the possibility to higher energy efficiency gains. The most effective core/shell nanocrystal combinations to optimize performance will be further investigated in future investigations. At the coming years, the photoelectrode will definitely have an even bigger influence on our day-to-day existence as additional nanomaterials and processes are developed. The cost of nanostorage capacity studies should also be reduced by using various nanomaterial preparation techniques.

**Conflicts of Interest:** The authors declare no conflict of interest.

**Funding:** No fund was received for this work.

#### References

- [1] Nayem, H.; Md., H. M.; Mariam, A. M.; Md, A. I.; Amran, H.; Fatema, T. Z.; Mohammad, A. C.; "Advances and Significances of Nanoparticles in Semiconductor Applications-A review". *Result. Eng.* 19: 101347, 2023.
- [2] Tehmeena, I.; Zainab, E.; Ayesha, Q.; Yasir, A.; Ali, I.; Sami, A.; Muhammad, A. I.; Magdi, E. A. Z.; "Recent Strategies to Improve the Photocatalytic Efficiency of TiO<sub>2</sub> for Enhanced Water Splitting to Produce Hydrogen". *Catalysts* 14: 674, 2024.
- [3] Sachin, R.; Sreejith, K.; Sandeep, V.; Hirendra, N. G.; "Effect of Surface States on Charge-Transfer Dynamics in Type II CdTe/ZnTe Core-Shell Quantum Dots: A Femto-second Transient Absorption Study". *J. Phys. Chem. C* 115: 12335–12342, 2024.
- [4] Jannik, R.; Hans, W.; Florian, J.; Marcel, D.; Yannic, U. S.; Christian, S.; Alf, M.; Tobias, K.; "Cation Exchange during the Synthesis of Colloidal Type-II ZnSe-Dot/CdS-Rod Nanocrystals". *Chem. Mater.* 35: 1238–1248, 2023.
- [5] Shilpa, G.; Mohan, P. K.; Kishore, K. D.; Deepthi, P. R.; Veera, S.; Anu, S.; Raghava, R. K.; "Recent Advances in the Development of High Efficiency Quantum Dot Sensitized Solar Cells (QDSSCs): A review". *Mater. Sci. Ener. Technol.* 6: 533-546, 2023.
- [6] Posudievsky, O. Y.; Konoshchuk, N. V.; Shkavro, A. G.; Koshechko, V. G.; Pokhodenko, V. D.; "Structure and Electronic Properties of Poly(3,4-ethylenedioxythiophene) Poly (styrene sulfonate) Prepared Under Ultrasonic Irradiation". *Synthetic Metals* 195: 335-339, 2023.
- [7] Hongbin, D.; Chunze, Y.; Ruixue, Z.; Lin, L.; Jihao, Z.; Tsu-Chien, W.; "Impact of Surface Trap States on Electron and Energy Transfer in CdSe Quantum Dots Studied by Femtosecond Transient Absorption Spectroscopy". *Nanomaterials* 14: 34, 2024.
- [8] Aizhao, P.; Lihe, Y.; Xiaoqin, M.; Youshen, W.; Yanfeng, Z.; Guijiang, Z.; Ling, H.; "Strongly Luminescent and Highly Stable Core-Shell Suprastructures from In-situ Growth of CsPbBr<sub>3</sub> Perovskite Nanocrystals in Multidentate Copolymer Micelles". *J. Allo. Comp.* 844: 156102. 2020.
- [9] Yang, M.; Anqiang, J.; Lei, K.; Jun, W.; Heng, G.; Sheng-Nian, L.; "Amplified Spontaneous Emission and Lasing from Zn-Processed AgIn<sub>5</sub>S<sub>8</sub> Core/Shell Quantum Dots". *ACS Appl. Mater. Interfaces* 15: 19330–19336, 2023.
- [10] Shahriar, M.; Sakineh, A. N.; Davood, A.; "Reduction of Recombination at the Interface of Perovskite and Elec-tron Transport Layer with Graded pt Quantum Dot Doping in Ambient Air-Processed Perovskite Solar cell". *Sci. Rep.* 14: 24254, 2024.
- [11] Kalpna, J.; Shyam, K.; Khundrakpam, S. S.; Michael, O.; Lavanya, M. R.; "Composition Related Tunability of "Green" Core/Shell Quantum Dots for Photovoltaic Applications from First Principles". *J. Phys. Chem. C* 125: 27046-27057, 2021.
- [12] Xi, W.; Peng, W.; Meng, L.; Jian, L.; "Advances in the Preparation and Biological Applications of Core@Shell Nanocrystals Based on Quantum Dots and Noble Metal". *RSC Adv.* 14: 26308–26324, 2024.
- [13] Zeina, A. A.; Falah, H. M.; "Two-Step Laser Ablation for the Synthesis of Au:Pb Core/Shell NPs for A high-Performance Silicon-Based Heterojunction Photodetector". *Iraqi J. Phys.* 22: 31-47. 2024.
- [14] Fariba, M. G.; Yong, Z.; Hongjie, A.; Nam-Trung, N.; "Core-Shell Microparticles: Generation Approaches and Applications". *Journal of Science: Advanced Materials and Devices*, 5, 417-435. 2020.
- [15] Ilya, V. C.; Aleksandra, D. R.; Alexander, G. K.; "Structure-Driven Tuning of Catalytic

- Properties of Core–Shell Nanostructures”. *Nanoscale* 16: 5870-5892, 2024.
- [16] Sourav, M.; Pranav, A.; Farazuddin, A.; Hirendra, N. G.; “Charge Carrier Dynamics in CdTe/ZnTe Core/Shell Nanocrystals for Photovoltaic Applications”. *J. Chem. Sci.* 130: 1-6, 2018.
- [17] Kadim, A. M.; Hammoodi, K. A.; Saleh, G. S.; “Fabrication of hybrid QDOLEDs from core/shell/shell QDs and conductive organic polymers”. *Nano Hybr. Compo.* 22: 11-22, 2018.
- [18] Kadim, A. M.; “White light generation from emissive hybrid nanocrystals CdSe/CdTe/CdS core/shell/shell system”. *Nano Hybr. Compo.* 27: 1-10, 2019.
- [19] Kadim, A. M.; “Fabrication of quantum dots light emitting device by using CdTe quantum dots and organic polymer”. *J. Nano Res.* 50: 48-56, 2017.
- [20] Kadim, A. M.; “Fabrication of nano battery from CdS quantum dots and organic polymer”. *Kuwait J. Sci.* 49: 1-9, 2022.